Princeton Plasma Physics Laboratory

PPPL- 4968

PPPL- 4968

Adaptive Grids In Simulations of Toroidal Plasma Starting From Magneto-hydrodynamic Equilibrium

Xujing Li, et. al.

DECEMBER, 2013

PPPL PRINCETON PLASMA PHYSICS LABORATORY

Prepared for the U.S. Department of Energy under Contract DE-AC02-09CH11466.

Princeton Plasma Physics Laboratory
Report Disclaimers

Full Legal Disclaimer

Trademark Disclaimer

PPPL Report Availability

Princeton Plasma Physics Laboratory:

http://www.pppl.gov/techreports.cfm

Office of Scientific and Technical Information (OSTI):

http://www.osti.gov/bridge

Related Links:

U.S. Department of Energy

Office of Scientific and Technical Information

Fusion Links

Adaptive grids in simulations of toroidal plasma starting from magneto-hydrodynamic equilibrium

X LI[1] and L E ZAKHAROV[2] and S A GALKIN[3]

[1]Institute of Computational Mathematics and Scientific/Engineering Computing, Academy of Mathematics and Systems Science, Chinese Academy of Sciences, Beijing, China. email: xli2@pppl.gov, t.n. +1-609-243-3580
[2]Princeton Plasma Physics Laboratory Princeton, New Jersey,US
[3]FAR-TECH, Inc. 10350 Science Center Dr. Bld 14, St 150, San Diego, CA 92121, USA,

Abstract. This paper introduces the notion of Tokamak Magneto-Hydrodynamics (TMHD), which explicitly reflects the anisotropy of the high temperature tokamak plasma. The set of TMHD equations is formulated for simulation of macroscopic plasma dynamics and disruptions in tokamaks. Free from the Courant restriction on the time step, this set of equations is adequate to plasma dynamics with realistic parameters of high performance plasmas and does not require any extension of the MHD plasma model. At the same time, TMHD requires the use of magnetic field aligned numerical grids. Examples of their use in 2-dimensional cases of tokamak equilibria and dynamics of the wall touching kink mode are presented. For the 3-dimensional case of ergodic magnetic field, this paper introduces the Reference Magnetic Coordinates as a practical algorithm for generating adaptive grids for TMHD.

Keywords: Tokamak, magneto-hydrodynamics, disruptions, numerical simulations, adaptive grid

PACS numbers: 02.60.Lj, 52.30.Bt, 52.55.Fa, 52.55.Hc

Submitted to: *Plasma Sci. and Technol.*

1. Introduction

Numerical methods always played a significant role in magnetic fusion research, a fact that motivated the development of innovative numerical schemes, specific for the high temperature plasmas. Magneto-hydrodynamics (MHD) of plasma[1] is a large part of plasma physics, where numerical methods are still evolving in order to address the emerging challenges in simulations of the high performance plasma of present and future devices.

The importance of different toroidal configurations for fusion is determined by two major properties:

(i) How macroscopically stable the plasma configuration is

(ii) How well does it confine particles and energy

The typical toroidal confinement devices are

(i) Stellarators, (3-dimensional, $B_{tor} \gg B_p,\ q \simeq 1$), are stable (no macroscopic MHD)

(ii) Tokamaks, (2-dimensional, $B_{tor} \gg B_p,\ q > 1$), are conditionally stable (disruptions are a problem[2])

(iii) Reversed Field Pinches, or RFP, ($B_{tor} \simeq B_p,\ q \ll 1$), are full of MHD activity

(iv) Spheromaks, ($B_{tor} \simeq B_p,\ q \simeq 1$), are full of MHD activity, short lived

(v) Field Reversed Configurations, FRC, ($B_{tor} \simeq 0,\ q = 0$), are MHD unstable (need energetic particle beams for stabilization)

Here, B_{tor}, B_p, q are the toroidal and poloidal magnetic fields, and the safety factor, correspondingly.

Regarding confinements, tokamaks have no rivals: 2-D (dimensional) tokamaks are consistent with the so-called Lithium Wall Fusion (LiWF) regime[3, 4, 5], uniquely suitable for fusion power. In this regime, which still remain to be developed, the plasma ions from the boundary are pumped out by the flowing liquid lithium. This prevents them from returning as cold neutral atoms back to the plasma edge and cooling down the plasma edge. As a result, the edge temperature is becoming comparable with the core temperature, while significantly enhanced confinement is determined by the core particle diffusion (rather than, as presently, by thermal conduction, which is always anomalously high).

The critical possibility of LiWF regimes makes tokamaks superior with respect to stellarators, despite the need for elimination of disruptions in tokamaks. Because of particle losses in their 3-D magnetic field, stellarators cannot utilize the LiWF regime at the same extend as tokamaks.

In this regard, tokamaks represent the special interest as a leader in fusion research with needs in simulations of macroscopic phenomena such as plasma equilibrium and disruptions. Being relatively benign in the earlier and present machines, the disruptions recently attracted a special attention because of their potentially big impact on design and future operation of the ITER device and other next step machines.

This paper describes the specifics of the macroscopic MHD in tokamaks and the needs in special numerical schemes, related to the dynamics of a highly anisotropic high temperature tokamak plasma. Now it is understood that new numerical schemes with grids aligned with the magnetic field have to be developed for simulation of tokamak disruptions and general MHD with realistic plasma parameters. The existing schemes, which are based on laboratory grids and are hydrodynamic in nature, cannot address the scale separation in the growing plasma anisotropy at enhanced plasma temperatures.

The tokamak plasma configurations during the stationary phase of the discharge are well described by classical equilibrium equations

$$\nabla p = (\vec{j} \times \vec{B}), \tag{1}$$

$$(\nabla \cdot \vec{B}) = 0, \tag{2}$$

$$(\nabla \times \vec{B}) = \mu_0 \vec{j}, \quad \mu_0 = 0.4\pi, \tag{3}$$

where p is the plasma pressure, $\vec{j}, \vec{B} = \vec{B}_p + \vec{B}_{tor}$ are the current density and magnetic field. In this paper we use the Units m (for lengths), T (for magnetic field), MA (for currents), MPa (for pressure), Vs (Volt-seconds, for magnetic fluxes).

Insensitive to the plasma model, the equilibrium equations serve as a basis of toroidal confinement: because of

$$(\vec{B} \cdot \nabla p) = 0 \tag{4}$$

plasma can be confined inside toroidal configurations if they have closed magnetic surfaces.

The needs in adaptive grids in equilibrium calculations were understood in the middle 1970s[6, 7, 8], and many tokamak equilibrium codes may exemplify the use of

adaptive, so-called flux coordinates. But even for this classical problem the adaptive grid approach had to be extended to the configurations limited by a separatrix.

This step was done recently by the authors[9] and described in Section II. It can be considered also as a preparation of a transition to the plasma dynamics of tokamaks, where force balance plays an exceptional role, which is not yet recognized to its full extent.

The first important characteristic of disruptions and other macroscopic MHD events in tokamaks is that their time scale is much shorter than the penetration time $\tau_{resistive}$ of the magnetic field into the plasma. This implies that the plasma dynamics preserves the magnetic fluxes and as a result excites localized currents of two types: surfaces currents at the plasma boundary, and the sheet currents at the resonant magnetic surfaces[10].

The second property is that in large machines the fastest phase in disruptions, called "thermal quench" (loss of plasma thermal energy), lasts about 1 ms, which is much longer than the characteristic inertia transit time τ_{MHD}. This implies that the plasma inertia, which is the driving term in existing numerical schemes, plays a minor role. Instead the electro-magnetic force balance plays a much bigger role.

The third characteristic of plasma dynamics in tokamaks is that the plasma flow to the wall is unrestricted, and the conventional hydro-dynamic boundary condition $V_{normal} = 0$ is not applicable for disruptions. The existing 3-D MHD codes, e.g., M3D[11] or NIMROD[12] imply this irrelevant restriction[13] to the high temperature plasma of tokamaks. Moreover, in the wrong plasma model of M3D code, the tokamak parameters are artificially adjusted in order to amplify a typically benign internal instability, thus, simulating the ITER device with 24 MA plasma current instead of its reference value of 15 MA[11].

In order to emphasize these specifics, we here introduce a special notion of Tokamak MHD (TMHD), which describes the macroscopic dynamics of the tokamak plasma as a fast equilibrium evolution with flux conservation and generation of localized currents in the plasma and the wall. It is based on the following time scale

relations, typical for tokamaks

$$\tau_{MHD} \simeq \frac{R}{V_A} = \underbrace{\frac{R}{2.18 \cdot 10^6 B_{tor}}}_{<1\ \mu s} \quad \ll \quad \underbrace{\tau_{TMHD}}_{\simeq 1\ ms} \ll \quad \underbrace{\tau_{transport}}_{\simeq 0.1\ s} \quad \ll \quad \underbrace{\tau_{resistive}}_{\simeq 1\ s}. \tag{5}$$

Here, R, V_A are the major plasma radius and Alfvén velocity, τ_{TMHD} is the low limit of events in the TMHD, $\tau_{transport}$ is the characteristic time of evolution of plasma parameters.

The paper is organized as follows. Section II gives numerical implementation of 2-D adaptive coordinates for tokamak equilibrium (ESC-EEC code system[9, 14]). The equations of TMHD are written in Section III with examples of numerical simulations of the Wall Touching Kink Mode (WTKM) Section IV introduces and describes the 3-D field aligned Reference Magnetic Coordinates (RMC) for ergodic magnetic fields together with an algorithm for generating and advancing RMC. The Summary specifies the near term needs in simulations of TMHD.

2. 2-D Grad-Shafranov equilibrium in tokamaks

The well known Grad-Shafranov (GSh) equation[15] describing tokamaks equilibrium ($\partial/\partial\phi = 0$) in cylindrical coordinates r, z, ϕ is represented by

$$\Delta^* \bar{\Psi} \equiv \frac{\partial^2 \bar{\Psi}}{\partial r^2} - \frac{1}{r}\frac{\partial \bar{\Psi}}{\partial r} + \frac{\partial^2 \bar{\Psi}}{\partial z^2} = -r^2 P(\bar{\Psi}) - T(\bar{\Psi}). \tag{6}$$

Here $\bar{\Psi} \equiv \Psi/(2\pi)$ and Ψ is the poloidal magnetic flux. Use the notation B_p and $B_\phi \equiv B_{tor}$ for poloidal and toroidal magnetic field respectively, the P and T in Eq. 6 have the following form

$$\vec{B} = \vec{B}_p + \vec{B}_\phi = \frac{1}{r}(\nabla \bar{\Psi} \times \vec{e}_\phi) + \frac{1}{r}\bar{F}(\bar{\Psi})\vec{e}_\phi, \tag{7}$$

$$\bar{F} = rB_\phi, \quad P(\bar{\Psi}) \equiv \mu_0 \frac{dp}{d\bar{\Psi}}, \quad T(\vec{\Psi}) \equiv \bar{F}\frac{d\bar{F}}{d\bar{\Psi}}. \tag{8}$$

The $r-z$ codes[16, 17] do not address the plasma anisotropy. Instead, we introduce the curvilinear coordinates[18] a, θ, ϕ, where a represents a radial coordinate, θ represents a poloidal angle and ϕ a toroidal angle, which are determined by

$$r = r(a, \theta), \quad z = z(a, \theta), \quad . \tag{9}$$

Then the Grad-Shafranov equation can be expressed as

$$\mathcal{L}\bar{\Psi} \equiv \frac{D}{r}\Delta^*\bar{\Psi} = -rDP - \frac{D}{r}T \tag{10}$$

where the linear operator

$$\mathcal{L} = \frac{\partial}{\partial a}\left(\frac{g_{\theta\theta}}{rD}\frac{\partial}{\partial a} - \frac{g_{a\theta}}{rD}\frac{\partial}{\partial \theta}\right) - \frac{\partial}{\partial \theta}\left(\frac{g_{a\theta}}{rD}\frac{\partial}{\partial a} - \frac{g_{aa}}{rD}\frac{\partial}{\partial \theta}\right) \tag{11}$$

and $D \equiv z'_a r'_\theta - z'_\theta r'_a$ is the 2-dimensional Jacobian, and $g_{aa}, g_{a\theta}, g_{\theta\theta}$ are the components of the metric tensor.

2.1. Linearized Grad-Shafranov equation

The fastest way of solving the non-linear GSh equation is by using its linearization[14], which can be outlined by

$$\bar{\Psi}(a,\theta) \qquad \equiv \bar{\Psi}^0(a) + \psi(a,\theta), \tag{12}$$

$$\Delta^*(\bar{\Psi}_0 + \psi) = -r^2 P(\bar{\Psi}_0 + \psi) - T(\bar{\Psi}_0 + \psi). \tag{13}$$

Here ψ is considered as a small perturbation, $\psi \ll \bar{\Psi}_0$ and is determined by the linearized GSh equation. Then, after linearization two equations follow

$$\begin{aligned} &\Delta^*\bar{\Psi}_0 = -r^2 P(a) - T(a), \\ &\Delta^*\psi + r^2\frac{dP}{d\bar{\Psi}}\psi + \frac{dT}{d\bar{\Psi}}\psi = 0. \end{aligned} \tag{14}$$

The alignment of the coordinates with the magnetic surfaces is achieved by the massaging toroidal surfaces in accordance with the equation

$$a \to a + \xi. \tag{15}$$

The displacement ξ is determined in an explicit form by

$$\bar{\Psi}(a+\xi,\theta) = \bar{\Psi}^0(a+\xi) + \psi(a,\theta) = \text{const}, \tag{16}$$

$$\xi = -\frac{\psi}{\bar{\Psi}'_0}. \tag{17}$$

Then, the coordinate system is adapted by a simple rule

$$r(a,\theta) \to r(a,\theta) + r'_a\xi, \quad z(a,\theta) \to z(a,\theta) + z'_a\xi. \tag{18}$$

Together with the linearized GSh equation, this gives a fast Newton scheme for solving non-linear GSh equation.

The equilibrium and stability code (ESC)[14] solves these linearized GSh equations using Fourier representations of $\psi, r(a,\theta), z(a,\theta)$.

2.2. Finite element method for the edge equilibrium

Since the Fourier representations cannot be extended to the boundary with a separatrix, the edge equilibrium code (EEC)[9] was developed specifically for the edge equilibrium simulation using finite element method. The solution of the GSh equation can be obtained by minimizing the energy functional

$$W = \frac{1}{2}\int \left\{ \frac{g_{\theta\theta}}{rD}\bar{\Psi}_a'^2 - 2\frac{g_{a\theta}}{rD}\bar{\Psi}_a'\bar{\Psi}_\theta' + \frac{g_{aa}}{rD}\bar{\Psi}_\theta'^2 \right. \\ \left. -2rD\bar{p}(\bar{\Psi}) - \frac{D}{r}\bar{F}^2(\bar{\Psi}) \right\} dad\theta + \oint_\Gamma \bar{\Psi} B_p^e dl, \tag{19}$$

e.g., using Hermite finite elements on the a, θ gird. Here, dl is the length element of the plasma boundary contour, and B_p^e is a given poloidal magnetic field at the plasma boundary.

The Hermite elements are exceptionally suitable for the simulations of equilibrium and TMHD: (a) the solution provides both unknown functions and their first derivatives, and (b) the resulting matrix equations has the block diagonal structure. For advancing the grid EEC uses the same algorithm as ESC. Both codes work as the ESC-EEC code system, where ESC calculates the plasma core equilibrium in the fastest manner, while EEC is applied for the boundary layer near the plasma boundary. The codes are interfaces through a virtual boundary and provide the continuity of magnetic flux and magnetic fields across it.

Examples of equilibrium calculations for different tokamak configurations calculated by ESC-EEC are shown in Fig.1.

In Fig. 1 the core plasma (blue region) equilibrium is calculated by ESC using a Fourier representation (β is the ratio of averaged plasma pressure to the pressure of the magnetic field). The edge equilibrium (red region) is calculated by EEC using Hermite elements. The continuity of magnetic fluxes and fields are provided through a virtual boundary.

The ESC-EEC code system with certain modifications is also suitable for implementation of TMHD for 2-D vertical instability and Vertical Displacement Event (VDE), which is a frequent kind of disruptions in tokamaks.

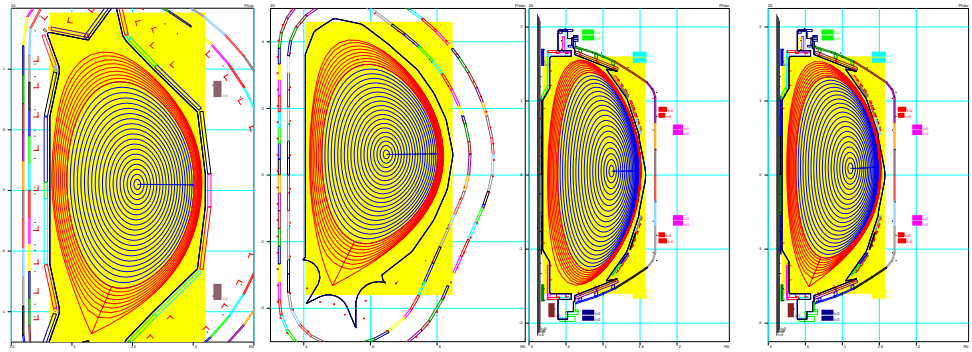

(a) $\beta = 2.5\%$ (b) $\beta = 6\%$ (c) $\beta = 35\%$ (d) $\beta = 33\%$

Figure 1. The examples equilibria of (a) EAST, (b) ITER, and NSTX high β (c) smooth boundary, and (d) boundary with an X-point.

3. Macroscopic tokamak MHD

If understood in a straightforward manner, MHD represents a hydrodynamics of conductive fluid with the Lorentz force $\vec{j} \times \vec{B}$ included into the equation of motion together with the Ampère and Faraday laws. Such an interpretation of MHD is consistent with dynamics of liquid metals in a magnetic field. With an appropriate model of plasma resistivity it might be applicable for MHD problems of RFP, Spheromaks and FRC.

The macroscopic tokamak TMHD is significantly different from MHD of liquid metals. Plasmas in tokamaks have a very high anisotropy. Since the electrons move much faster along the magnetic field lines than across the field lines, the electron temperature is almost constant along the field lines, i.e.,

$$(\vec{B} \cdot \nabla T_e) \simeq 0, \tag{20}$$

and this condition is becoming more valid at high temperature of contemporary and future tokamaks.

Since the electric conductivity is a function of electron temperature $\sigma = \sigma(T_e)$,

$$(\vec{B} \cdot \nabla \sigma) = 0. \tag{21}$$

This condition is an adequate form for expressing the tokamak plasma anisotropy. In contrast, the existing numerical codes, which are incapable to implement it explicitly, introduce additional anisotropic thermal conduction equation for T_e [11, 12]. Not only

this equation is not a part of MHD, the perpendicular thermal conductivity is one of the major unknowns in tokamak plasma, while a realistic parallel thermal conduction cannot be reproduced by laboratory numerical grids.

At the same time the TMHD model of resistivity does not cause problems for the adaptive grids a, θ, φ, aligned with the magnetic field, in which $\sigma = \sigma(a)$.

Unlike dynamics of liquid metals, which needs the boundary condition on normal velocity at the solid surfaces in all existing 3-D plasma physics MHD codes,

$$V_{normal} = 0, \tag{22}$$

in reality, there is no restriction on the tokamak plasma flow to the wall. Plasma ions can go to the wall, where they are converted into a neutral atoms, which do not participate anymore in plasma dynamics. As a result, there is absorption of the plasma by the wall, significant for the tokamak plasma dynamics.

The third key difference of TMHD from the present hydrodynamic interpretation and implementation of plasma MHD is related to the inertia term in the equation of motion

$$\rho \frac{d\vec{V}}{dt} = -\nabla p + (\vec{j} \times \vec{B}). \tag{23}$$

The inertia term, which serves as a driver of MHD dynamics in existing codes, is related to several so far unresolved problems, preventing realistic simulations of tokamaks.

Fast magneto-sonic waves, which play a negligible role in tokamaks, require a very small time step due to Courant condition. In fact, the macroscopic tokamak plasma dynamics is driven by a small imbalance of forces, which are much bigger than the plasma inertia and are reflected in time scales (5).

Instead of inertial motion, the macroscopic TMHD is, in fact, a fast equilibrium evolution with excitation of sheet currents or islands at the resonant surfaces and surface currents at the plasma boundary due to magnetic flux conservation ($\tau_{TMHD} \ll \tau_{resistive}$). Because of this relation, existing numerical schemes are not suitable for TMHD and are more relevant to much less stable RFP and spheromaks, rather than to tokamaks.

In TMHD, following Kadomtsev and Pogutse[19], the plasma inertia is replaced by a displacement term, which is equivalent to a friction force $\propto -\vec{V}$, opposite in sign to velocity,

$$\lambda\delta\vec{r} = -\nabla p + (\vec{j}\times\vec{B}), \quad \lambda\delta\vec{r} \equiv \gamma\vec{V}, \tag{24}$$

where γ, λ play the role of relaxation parameters in the fast evolving sequence of equilibria.

This replacement provides an iteration algorithm relevant to TMHD for driving the system. By eliminating plasma oscillations it removes the 4-decade old problem with Courant limitations on the time step in MHD simulations.

Based on these considerations, the basic set of equations which can address the nature of macroscopic TMHD is represented by

$$\lambda\delta\vec{r} = -\nabla p + (\vec{j}\times\vec{B}), \tag{25}$$

$$\vec{B} = (\nabla\times\vec{A}), \quad \mu_0\vec{j} = (\nabla\times\vec{B}), \tag{26}$$

$$-\frac{\partial\vec{A}}{\partial t} - \nabla\varphi_E + (\vec{V}\times\vec{B}) = \frac{\vec{j}}{\sigma}, \quad (\vec{B}\cdot\nabla\sigma) = 0 \tag{27}$$

$$\vec{V} \equiv \frac{\partial\delta\vec{r}}{\partial t}, \quad (\nabla\cdot\vec{V}) = 0 \tag{28}$$

Here the notations are: $\vec{j}$ is the current density, p is the plasma kinetic pressure, $\vec{B}$ is the magnetic field, $\vec{A}$ and φ_E are the magnetic and electric potential, respectively, and $\vec{V}$ is the plasma velocity. These equations have to be complemented by the conventional circuit equations for the currents in the wall.

Summarizing the distinction with the conventional MHD, in this set of equations, the inertia term $\rho d\vec{v}/dt$ is replaced by an effective "friction", $\lambda\delta\vec{r}$. The plasma anisotropy is expressed explicitly by $(\vec{B}\cdot\nabla\sigma) = 0$. Plasma velocity is a secondary variable and can be calculated by the rate of displacement. As a result, the plasma is allowed to flow into the wall with no special restrictions.

Fig. 2 gives an example of implementation of TMHD for simulation of an instable Wall Touching Kink Mode [20, 10] in 2-D approximation of a plasma with a circular cross section ($R \gg a$, R, a are the major and minor radii of the plasma) in a strong magnetic field $B_{tor} \gg B_p$. The safety factor $q \equiv aB_{tor}/(RB_p)$ in simulations is taken

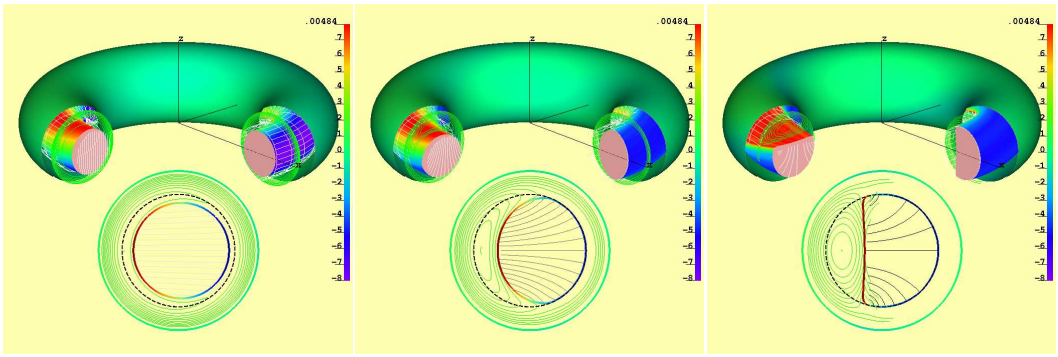

(a) (b) (c)

Figure 2. Fast phase of WTKM instability. (a) Initial small helical perturbation of an unstable plasma; (b) Plasma boundary hits the tile surface and generate Hiro currents; (c) Plasma reaches an equilibrium maintained by Hiro currents.

as $q = 0.75$. The plasma is situated inside a super-conducting wall (green). In the vacuum region there is a toroidal surface, which consists of conducting, but insulated from each other, tiles. This model reflects a typical in-vessel environment of tokamaks. The part of the tile surface, which is not touched by the plasma, is transparent to the evolving magnetic filed. On the other hand, the zone where the plasma touches the tiles is simulated as super-conducting.

The numerical mesh is conformal to the plasma boundary, which is well reproduced at all stages. Under the assumptions of the model the unstable plasma moves fast initially, but slows down after touching the tile surface without penetration into it. Finally the new equilibrium, supported by the currents in the tile surface (called Hiro currents), is reached (the right frame).

Fig. 3 shows the following evolution of the WTKM due to resistive decay of the Hiro currents in the tile surface. The plasma keeps its macroscopic equilibrium by moving into the tiles and, thus, maintaining the necessary level of Hiro currents. Finally, the plasma disappears.

This simple illustrative 2-D model of plasma dynamics in tokamak disruptions, which was simulated using adaptive grids, cannot be reproduced by the existing 3-D numerical codes, which miss the most important effect of Hiro currents and plasma

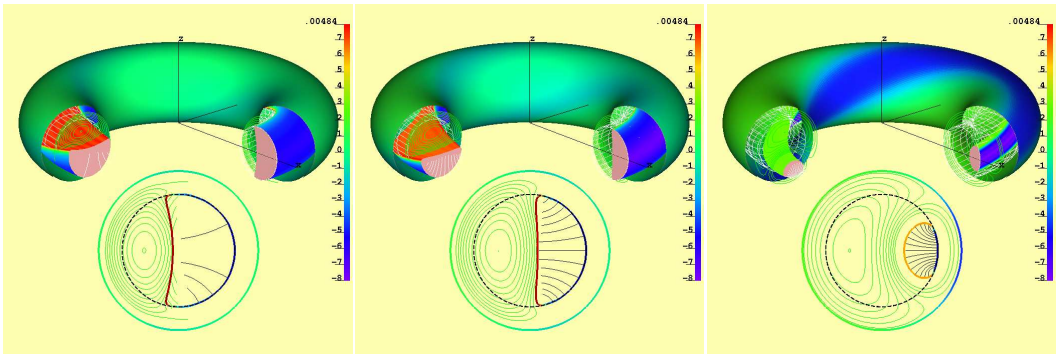

(a) (b) (c)

Figure 3. Fast equilibrium evolution due to decay of the Hiro currents. (a) Initial plasma penetration into the wall; (b) Shrinking of the plasma cross-section; (c) The latest stage of plasma disappearance.

disappearance in the wall.

Simple at the first glance, the TMHD equations (25-28) cannot be reproduced by numerical schemes based on laboratory coordinate systems. New schemes, based on adaptive coordinates aligned with the magnetic field are required by TMHD.

The next section addresses the fundamental problem of adaptive coordinates in 3-D magnetic fields, which is related to formation of islands on the resonant magnetic surfaces and stochastic regions even by small magnetic perturbations.

4. 3-D Ergodic magnetic fields and RMC

The ESC-EEC code system addresses essentially all typical tokamak 2-D equilibrium problems, including reconstruction and variance analysis [21, 22, 23]. Its algorithm relies on the existence of magnetic surfaces $\bar{\Psi}$ =const. On the other hand, in 3-D configurations, there are no $\bar{\Psi}$ =const-like equation, which would be useful for generation of adaptive numerical grids. This creates difficulties in simulation of 3-D plasma even for its equilibrium.

The conventional practices of revealing the topology of the magnetic field rely on "line tracing" by solving the equation for magnetic field lines

$$\frac{d\vec{r}}{dl} = \frac{\vec{B}}{|\vec{B}|}. \tag{29}$$

But this approach is very time consuming for the reconstruction of magnetic surfaces

with the use of Poincare plots even in the cases when the magnetic surfaces do exist. The existence of resonant surfaces makes Poincare plots not representative for magnetic surfaces. Moreover, when the magnetic field is ergodic, the line tracing gives no clue on designing working coordinate surfaces. Also, the line tracing cannot resolve small islands and plasma dynamics near the resonant surfaces.

Here, we describe a different and practical method of aligning toroidal coordinates with the ergodic magnetic field. Then these coordinates can be used for generating numerical grids for TMHD in 3D magnetic fields.

4.1. Reference Magnetic Coordinates

In 3-D toroidal coordinates a, θ, ϕ, the general form of vector potential $\vec{A}$ has the form

$$\begin{aligned}\vec{A} = & -\eta(a,\theta,\phi)\nabla a + \bar{\Phi}(a,\theta,\phi)\nabla\theta \\ & + \bar{\Psi}(a,\theta,\phi)\nabla\phi + \nabla u,\end{aligned} \tag{30}$$

where η is the radial component, depending on the choice of angles θ, ϕ, $\bar{\Phi}$ is the toroidal flux, and u is an arbitrary function.

We introduce here useful notations for 3-D functions, e.g., $u(a,\theta,\phi)$, reflecting their dependence on angles,

$$u(a,\theta,\phi) \equiv u_{00}(a) + u_{0\sim}(a,\phi) + u_{\sim\sim}(a,\theta,\phi), \tag{31}$$

where the first subscript corresponds to θ, and the second to ϕ, and

$$u_{00}(a) = \frac{1}{4\pi^2}\oint\oint u(a,\theta,\phi)d\theta d\phi, \tag{32}$$

$$\oint u_{0\sim}(a,\phi)d\phi = 0, \tag{33}$$

$$\oint u_{\sim\sim}(a,\theta,\phi)d\theta = \oint u_{\sim\sim}(a,\theta,\phi)d\phi = 0. \tag{34}$$

Then in the similar representation of $\bar{\Phi}$

$$\bar{\Phi}(a,\theta,\phi) \equiv \bar{\Phi}(a) + \varphi(a,\phi) + \varphi_{\sim\sim}(a,\theta,\phi). \tag{35}$$

The last term can be eliminated by choosing

$$u_{\theta,\sim\sim} \equiv -\varphi_{\sim\sim}(a,\theta,\phi). \tag{36}$$

In its turn, in the representation of $\bar{\Psi}$

$$\bar{\Psi}(a,\theta,\phi) \equiv \bar{\Psi}(a) + \psi_{0\sim}(a,\phi) + \psi_{\sim\sim}(a,\theta,\phi) \tag{37}$$

the second term can be eliminated by an additional term in u

$$u_{\phi,0\sim} \equiv -\psi_{0\sim}(a,\phi). \tag{38}$$

This results in the simplest representation of the vector potential in arbitrary toroidal coordinates

$$\begin{aligned}\vec{A} = & -\eta(a,\theta,\phi)\bar{\Phi}'(a)\nabla a + [\bar{\Phi}(a) + \varphi(a,\phi)]\nabla\theta \\ & + [\bar{\Psi}(a) + \psi(a,\theta,\phi)]\nabla\phi.\end{aligned} \tag{39}$$

Now the goal is to massage the toroidal coordinates in order to eliminate the normal component of magnetic field to the $a = const$ surface. Assuming, that the system is advanced by

$$a \to a + \xi \tag{40}$$

the condition of elimination of the radial magnetic field is

$$\vec{B} \cdot \nabla(a + \xi) = 0. \tag{41}$$

The linearized version of this equation, assuming that the oscillatory terms φ, ψ in vector potential are small compared to the averaged terms $\bar{\Phi}, \bar{\Psi}$ represents the magnetic differential equation for ξ

$$(\bar{\Psi}' - \bar{\Phi}'\eta'_\phi)\xi'_\theta - \bar{\Phi}'(1 - \eta'_\theta)\xi'_\phi = \psi'_\theta - \varphi'_\phi. \tag{42}$$

This equation can be easily solved in Fourier space

$$\begin{aligned}\xi &= \sum \xi_{mn}(a)e^{im\bar{\theta}-in\phi}, \quad \bar{\theta} = \theta - \eta, \\ \psi &= \sum \psi_{mn}(a)e^{im\bar{\theta}-in\phi}, \\ \varphi &= \sum \varphi_n(a)e^{-in\phi}.\end{aligned} \tag{43}$$

This gives

$$\xi'_\theta = \sum \xi_{mn}e^{im\bar{\theta}-in\phi}im(1 - \eta'_\theta), \tag{44}$$

$$\xi'_\phi = \sum \xi_{mn}e^{im\bar{\theta}-in\phi}(-im\eta'_\phi - in), \tag{45}$$

which after substitution into the equation (42) leads to a simple relation

$$(m\bar{\Psi}' + n\bar{\Phi}')\xi_{mn} = m\psi_{mn} - \delta^0_m n\varphi_n, \tag{46}$$

with Kronecker delta δ^0_m. This equation for ξ_{mn} can be resolved for all non-resonant harmonics m', n' for which the factor in front of ξ_{mn} is not zero.

Now the coordinate surfaces can be advanced exclusively by non-resonant components in ξ, which have the explicit form

$$\xi \quad = \sum_{m'n'} \xi_{m'n'}(a) e^{im'\bar{\theta} - in'\phi}, \tag{47}$$

$$\xi_{m'n'} = \frac{m'\psi_{m'n'} - \delta^0_m n\varphi_n}{m'\bar{\Psi}' + n'\bar{\Phi}'}, \tag{48}$$

ignoring resonant terms.

As a result of successive application of this algorithm, the coordinate system is deformed in a such way, that the vector potential acquires the simplest representation, achievable without massaging the angles of coordinates.

$$\begin{aligned}\vec{A} = & -\eta(a,\theta,\phi)\bar{\Phi}'(a)\nabla a + \bar{\Phi}(a)\nabla\theta \\ & + [\bar{\Psi}(a) + \psi^*(a,\theta,\phi)]\nabla\phi.\end{aligned} \tag{49}$$

$$\psi^* = \sum_{m^*n^*} \xi_{m^*n^*}(a) e^{im^*\bar{\theta} - in^*\phi}, \tag{50}$$

where ψ^* contains only resonant terms. Note, that by changing the definition of one of the angles, e.g., θ the η term in the vector potential can be eliminated as well, thus, making the representation of $\vec{A}$ similar to the 2-D straight field coordinates form. Typically this procedure leads to highly non-uniform distribution of θ =const lines, which makes such "quasi-straight field" coordinates impractical for simulations.

We call the resulting coordinate system Reference Magnetic Coordinate, or RMC, which is a proper substitution for the the flux coordinates in 3-D case.

The elimination of resonant terms is not possible without change in the topology of coordinates. At the same time, the RMC can be optimized in an obvious way by leaving the resonant harmonics in ψ^* localized radially within their island size w_{mn}. It can be derived to be equal to

$$w_{mn} = 4\sqrt{\left|\frac{m\psi^*_{mn}}{\bar{\Phi}'\iota'}\right|}, \quad \iota \equiv -\frac{\bar{\Psi}'}{\bar{\Phi}'}. \tag{51}$$

Although, the topology of RMC does not correspond to the topology of the magnetic field, the magnetic topology can be easily reconstructed by the perturbation method, using the island size as an expansion parameter. In the simple case, when there is no radial overlapping of the resonant harmonics, it is determined near the resonant surface similarly to the 2-D case

$$\bar{\Psi}^*_{nm}(a,\theta,\phi) \equiv n\bar{\Phi}' + m\bar{\Psi}' + \left(\psi^*_{mn} e^{im\bar{\theta}-in\phi} + c.c.\right) = \text{const}, \tag{52}$$

by introducing of a local flux function $\bar{\Psi}^*$. It is possible to extend the perturbation theory on either a more general case or to include higher order terms.

The size of the resulting islands gives a self-contained condition of applicability of the perturbation theory.

The described coordinate advancing scheme, which leads to RMC, is analogous to the 2-D scheme of ESC for the fast and explicit advancing of the numerical mesh. It is remarkable that generation of field aligned RMC for ergodic magnetic fields has a simple and fast Newton scheme.

Fig. 4 shows an example of calculation of an early version of the W-7X vacuum field. Four representative toroidal cross sections of one of 5 toroidal periods are shown. The black points in the figure are Poincare points from the line tracing. The red lines are 3-D reference magnetic coordinates generated within 1 sec on an early (1998) Sun workstation.

5. Summary

After 62 years (since 1951 and Shafranov's stability criterion[24], $q > 1$), there are still no numerical codes addressing properly the macroscopic tokamak MHD. For decades, the existing 3-D numerical codes have been suffering from Courant restrictions on the time step, and are not capable to reproduce the exceptionally high tokamak plasma anisotropy, while relying on extensions of MHD model by introducing the unreliable heat conduction equation, essentially to hide the problem. In addition, the boundary condition $V_{normal} = 0$on solid surfaces, irrelevant to high temperature plasma does

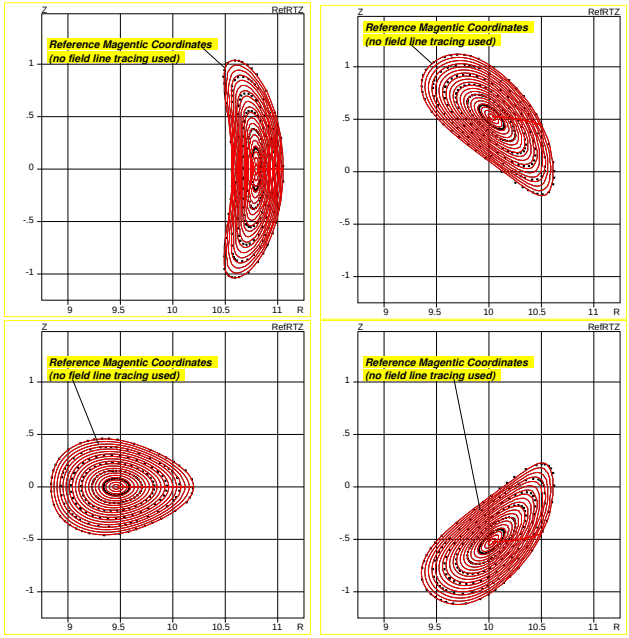

Figure 4. Vacuum magnetic surfaces of a 3-D magnetic configuration with 5 toroidal periods (as in W7X stellarator).

not allow to simulate disruption events in tokamaks.

Instead, this paper introduces the specific Tokamak MHD, which describes well the plasma anisotropy within the MHD model. It does not require its unjustified extension for simulating macroscopic instabilities and disruptions. TMHD requires adaptive grids, aligned with the magnetic field. For 2-D cases, including the vertical instability and disruptions, such a scheme is already developed and tested in equilibrium calculations.

For 3-D plasma dynamics, which involves ergodic magnetic fields, this paper has introduced the Reference Magnetic Coordinates, with the best possible alignment of simple nested toroidal surfaces to the 3-D magnetic field. RMC give a fast Newton scheme for the generation of adaptive grids in the case of 3-D TMHD.

TMHD also covers the stellarator needs in equilibria: up to now, the simulations of stellarator configurations lack the implementation of the Hamada condition (1960), which is the key confinement principle for 3-D configurations. Application of TMHD algorithms will allow to fulfill the Hamada condition in 3-D equilibrium calculations

in the most effective fashion.

Acknowledgments

This work is partially supported by US DoE contract No. DE-AC02-09-CH11466, by the Chinese National Magnetic Confinement Fusion Science Program 2011GB105003, and by the US DOE SBIR grant # 94307S10-II

References

[1] J.P. Freidberg. 1987, "Ideal Magnetohydrodynamics (Modern Perspectives in Energy)". Plenum Press: New York, London
[2] E. P. Gorbunov, K. A. Razumova. 1963, Atomnaya Energia, **15**: 363
[3] S. I. Krasheninnikov, L. E. Zakharov, G. V. Pereverzev. 2003, Phys. of Plasmas, v. 10: 1678
[4] L. E. Zakharov. 2011, Journal of Nuclear Science and Technology, Fusion Series, (`http://vant.iterru.ru/vant_2011_1.htm`) #1: 29
[5] L. E. Zakharov. 2011, Journal of Nuclear Science and Technology, Fusion Series, (`http://vant.iterru.ru/vant_2011_1.htm`) #3: 27
[6] P. Vabishevich, L. M. Degtyarev, and A. P. Favorski. 1978, Soviet Journal of Plasma Physics **4**: 554
[7] L. M. Degtyarev and V. V. Drozdov. 1985, Computer Physics Reports, **2**: 341
[8] L. M. Degtyarev and V. V. Drozdov. 1991, International Journal of Modern Physics C, **2**: 30
[9] X. Li, L.E. Zakharov. 2013, Submitted to Physics of Plasmas
[10] L.E. Zakharov, S.A. Galkin, S.N. Gerasimov, and JET-EFDA contributors. 2012, Phys. of Plasmas, **19**: 055703
[11] H. R. Strauss, R. Paccagnella, and J. Breslau. 2010, Phys. of Plasmas, **17**: 082505
[12] C. R. Sovinec, A. H. Glasser, T. A. Gianakon, D. C. Barnes, R. A. Nebel, S. E. Kruger, D. D. Schnack, S. J. Plimpton, A. Tarditi, M. S. Chu the NIMROD Team. 2004, J. of Comput. Phys., **195**: 355
[13] L. E. Zakharov. Phys. of Plasmas, 2010, **17**: 124703
[14] L. E. Zakharov and A. Pletzer. 1999 Phys. of Plasmas, **6**: 4693
[15] V. D. Shafranov. 1966, *Reviews of Plasma Physics*. Consultant Bureau: New York, Vol. 2: 103
[16] L. L. Lao, H. St. John, R. D. Stambaugh, A. G. Kellman, and W. Pfeiffer, 1985, Nucl. Fusion, **25**: 1611
[17] L. L. Lao, J. R. Ferron, R. J. Groebner, W. Howl, H. St. John, E. J. Strait, and T. S. Taylor. 1990, Nucl. Fusion, **30**: 1035
[18] L. E. Zakharov and V. D. Shafranov. in Reviews of Plasma Physics, edited by Acad. M. A. Leontovich (Consulant Bureau, New York, 1986), Vol. 11: 153
[19] B.B. Kadomtsev, O.P. Pogutse. 1977, Zh. Eksp. Teor. Fiz., **65**: 575
[20] L. E. Zakharov. 2008, Phys. of Plasmas, **15**: 062507
[21] L.E. Zakharov, E.L. Foley, F.M. Levinton, and H. Y. Yuh. 2008, Plasma Phys. Rep. **34**: 173
[22] L.E. Zakharov, J. Lewandowski, E.L. Foley, F. M. Levinton, H.Y. Yuh, V.V. Drozdov, D.C. McDonald. 2008, Phys. of Plasmas, **15**: 092503

[23] E.L. Foley, F.M. Levinton, H. Y. Yuh, and L.E. Zakharov. 2008, Nucl. Fusion **48**: 085004

[24] M. A. Leontovich, V. D. Shafranov. 1961, *Plasma Physics and the Problem of Controlled Thermonuclear Reactions*, edited by Acad. M. A. Leontovich, (Pergamon Press, New York-Oxford-London-Paris) Vol.1: 255

The Princeton Plasma Physics Laboratory is operated
by Princeton University under contract
with the U.S. Department of Energy.

Information Services
Princeton Plasma Physics Laboratory
P.O. Box 451
Princeton, NJ 08543

Phone: 609-243-2245
Fax: 609-243-2751
e-mail: pppl_info@pppl.gov
Internet Address: http://www.pppl.gov